Acta Crystallographica Section D
Biological Crystallography
ISSN 0907-4449

Anti-TRAP protein from *Bacillus subtilis*: crystallization and internal symmetry

Mikhail B. Shevtsov,[a] Yanling Chen,[b] Paul Gollnick[b] and Alfred A. Antson[a]*

[a]York Structural Biology Laboratory, Chemistry Department, York University, York YO10 5YW, England, and [b]Department of Biological Sciences, State University of New York at Buffalo, New York 14260, USA

Correspondence e-mail: fred@ysbl.york.ac.uk

Received 5 March 2004
Accepted 8 May 2004

Anti-TRAP protein regulates the expression of tryptophan biosynthetic genes by binding to TRAP and preventing formation of the TRAP–RNA complex. Anti-TRAP from *Bacillus subtilis* has been crystallized by vapour diffusion. The crystals belong to space group $P1$, with unit-cell parameters $a = 51.6$, $b = 60.1$, $c = 60.4$ Å, $\alpha = 114.0$, $\beta = 101.4$, $\gamma = 100.5^\circ$. X-ray data have been collected to 2.8 Å resolution. Peaks in the self-rotation function correspond to four trimers in the unit cell related by twofold and threefold rotational axes. The symmetry and gel-filtration data suggest that the protein exists as a trimer or a dodecamer in solution.

1. Introduction

Bacillus subtilis anti-TRAP regulates the expression of tryptophan biosynthetic genes by binding to the *trp* RNA-binding attenuation protein (TRAP; Valbuzzi & Yanofsky, 2002) and preventing interaction of TRAP with RNA by masking its binding site (Valbuzzi *et al.*, 2002). In the absence of anti-TRAP, TRAP, when activated by bound L-tryptophan, binds to the mRNA region within the 5′ leader region of the *trpECDFBA* operon, resulting in the formation of a transcription-termination hairpin (Gollnick, 1994; Babitzke & Gollnick, 2001, 2002). The RNA-binding segment is organized as 11 (G/U)AG repeats separated by two or three variable 'spacer' nucleotides (Babitzke *et al.*, 1994, 1995). TRAP also regulates the translation of several genes by binding to specific regions of mRNAs (Merino *et al.*, 1995). Expression of anti-TRAP protein is induced by the accumulation of uncharged $tRNA^{Trp}$ in the cell (Valbuzzi & Yanofsky, 2001). Therefore, regulation of tryptophan synthesis in *B. subtilis* occurs by sensing both the level of charged $tRNA^{Trp}$ and the level of free cellular tryptophan.

Anti-TRAP is a small oligomeric protein (5.6 kDa) composed of several identical 53-amino-acid polypeptides (Valbuzzi & Yanofsky, 2001). Each monomer binds one Zn atom, which is essential for its activity; removal of zinc converts anti-TRAP to inactive monomers (Valbuzzi & Yanofsky, 2002). The amino-acid sequence of anti-TRAP shows some homology to the cysteine-rich domain of the chaperone protein DnaJ (Valbuzzi & Yanofsky, 2001), the sequence identity for residues segment 9–39 containing two cysteine-rich motifs being 32%. The cysteine-rich motif C*XX*C*X*G*X*G (where *X* represents a variable amino acid) is repeated four times in DnaJ and appears twice in anti-TRAP. The NMR structure of DnaJ (Martinez-Yamout *et al.*, 2000) showed that two such motifs are involved in binding one Zn atom, with four cysteine side chains coordinated to the metal. Substitution of any anti-TRAP cysteine residue by alanine results in rapid degradation of the mutant proteins *in vivo* (Valbuzzi & Yanofsky, 2002). Chemical cross-linking experiments have suggested that anti-TRAP exists as a hexamer composed of two identical trimers. Within the trimer, subunits appear to be bound *via* Zn atoms, with the metal atom coordinated by four cysteine residue side chains: two from one subunit and two from an adjacent subunit (Valbuzzi & Yanofsky, 2002).

It has recently been shown by analytical ultracentrifugation that anti-TRAP exhibits concentration-dependent and reversible self-association. Experiments, which were performed over the concentration range 12.5–214 μ*M*, indicated that most of the protein exists as a trimer at low concentration and as a dodecamer at high concentration (Snyder *et al.*, 2004).

The three-dimensional structures of tryptophan-activated TRAP (Antson *et al.*, 1995; Chen *et al.*, 1999) and of several TRAP–RNA complexes have been determined (Antson *et al.*, 1999; Hopcroft *et al.*, 2002). TRAP is a toroid-shaped molecule composed of 11 identical subunits with 11 tryptophan-binding sites located at subunit–subunit interfaces. Tryptophan binding stabilizes the active conformation of TRAP, enabling it to interact with RNA (McElroy *et al.*, 2002). In the TRAP–RNA complex, the RNA chain binds to 11 binding sites, forming a belt around the protein molecule.

To date, there is no structural information available for anti-TRAP. Here, we describe the crystallization of anti-TRAP from *B. subtilis*.

© 2004 International Union of Crystallography
Printed in Denmark – all rights reserved

We also describe preliminary X-ray data analysis, which suggests the possible internal symmetry of anti-TRAP.

2. Material and methods

2.1. Overexpression and purification of anti-TRAP

Anti-TRAP was purified by a modification of the procedure described by Valbuzzi & Yanofsky (2001). Anti-TRAP was expressed using the T7 expression system and pET17b (Novagen). The resulting plasmid was transformed into *Escherichia coli* Rosetta (DE3) competent cells (Novagen). Cells were grown in LB medium until early log phase (A_{600} = 0.4), at which point anti-TRAP expression was induced by addition of 1 m*M* isopropyl-1-thio-β-D-galactopyranoside and the cells were grown for an additional 3 h. Cells were collected by centrifugation and broken in a French Pressure cell (Aminco) in buffer *A* (100 m*M* Tris–HCl pH 7.8, 1 m*M* dithiothreitol). Cell debris was removed by centrifugation at 30 000*g* for 20 min. Streptomycin sulfate was added to the supernatant to 3%(*w*/*v*), with stirring on ice for 20 min, and the precipitate was removed by centrifugation as above. The supernatant was heated at 363 K for 8 min and the insoluble proteins were removed by centrifugation. Anti-TRAP is a thermostable protein and on heating the extract most (>90%) of the *E. coli* proteins are denatured and precipitate but anti-TRAP does not. The supernatant was dialysed overnight against buffer *B* (50 m*M* Tris–HCl pH 7.8, 1 m*M* dithiothreitol) and then loaded onto a MonoQ Sepharose column (Pharmacia) equilibrated with buffer *B*. Anti-TRAP was eluted with a 0–1.0 *M* NaCl gradient and the fractions containing anti-TRAP were collected and concentrated using an Amicon Ultra-15 (Millipore) device. After dialysis overnight against buffer *A*, the sample was passed over a Sephadex G-75 column equilibrated with buffer *A*. Anti-TRAP fractions were pooled and concentrated as above. The purity of the anti-TRAP was monitored by SDS gel electrophoresis and its concentration was determined by BCA protein assay (Pierce).

2.2. Gel filtration

Gel-filtration experiments were performed using a Superdex-200 column with a total elution volume of 120 ml. The column was equilibrated with 5 m*M* triethanolamine pH 8.0, 20 m*M* NaCl, 1 m*M* dithiothreitol and calibrated using standard protein molecular-weight markers. The protein concentration used was 1 mg ml^{-1}, with an overall sample volume of 1 ml. The flow rate during the column run was 1 ml min^{-1}. Because of the absence of tryptophan residues and the presence of only a single tyrosine residue (one per monomer), the elution profile of the protein was monitored at 215 nm.

2.3. Crystallization

Anti-TRAP protein was dialysed against a solution containing 1 m*M* dithiothreitol, 20 m*M* NaCl and 5 m*M* triethanolamine pH 8.0 and concentrated to 15 mg ml^{-1} using an ultrafiltration membrane (Filtron). The protein concentration was estimated using the Bradford reagent (Pierce) with bovine serum albumin as standard (Bradford, 1976).

Crystals of anti-TRAP were grown using hanging-drop vapour diffusion (McPherson, 1982). Initial screening was performed using sparse-matrix kits from Hampton Research (Jancarik & Kim, 1991). The protein solution was allowed to equilibrate against 0.5 ml of reservoir solution at 293 K. Each droplet was formed by mixing equal volumes (1 µl) of protein solution and reservoir solution. After the initial crystallization trials, the best conditions were optimized.

2.4. X-ray data collection

For the diffraction experiment, crystals were flash-frozen in a cryosolution composed of crystallization ingredients with a slightly higher concentration of precipitating agent (PEG) and with the addition of 16%(*v*/*v*) glycerol. X-ray data were collected at 110 K and a wavelength of 0.87 Å using synchrotron radiation at beamline 9.6 (Daresbury) and an ADSC Quantum 4 CCD detector. During the experiment, the oscillation angle was 1.0°, the crystal-to-detector distance was 300 mm and the exposure time per oscillation was 80 s with three oscillations per image. A total of 183 images were collected. Diffraction data were integrated using *MOSFLM* (Leslie, 1993) and scaled and merged with *SCALA* (Evans, 1997). All crystallographic calculations were performed using the *CCP*4 suite of programs (Collaborative Computational Project, Number 4, 1994). The self-rotation function was calculated using *MOLREP* (Vagin & Teplyakov, 1997).

3. Results and discussion

3.1. Gel filtration

Two peaks were observed on the gel-filtration profile: one major peak, which is consistent with a weight of about 65 kDa, and a second less abundant peak with a weight corresponding to 16 kDa. The weight of one anti-TRAP monomer is ∼5.6 kDa. Therefore, the first peak in the gel-filtration profile probably corresponds to a dodecamer (67.2 kDa) and the second peak corresponds to a trimer (16.8 kDa) (Fig. 1).

3.2. Crystals of anti-TRAP

The best crystals of anti-TRAP were obtained with a reservoir containing 21–23%(*w*/*v*) poly(ethylene) glycol 5000 monomethyl ether, 0.1 *M* sodium cacodylate pH 6.5 and 50 m*M* magnesium acetate. Plate-shaped crystals with approximate dimensions of 0.4 × 0.1 × 0.05 mm grew in 3–4 d (Fig. 2*a*). These crystals proved to be anisotropic and highly mosaic (1–2°), with several plates often grown into each other. These crystals belonged to space group *P*1, with unit-cell parameters a = 51.6, b = 60.1, c = 60.4 Å, α = 114.0, β = 101.4, γ = 100.5°. A total of more than 50 crystals were tested before one single crystal diffracting to 3 Å

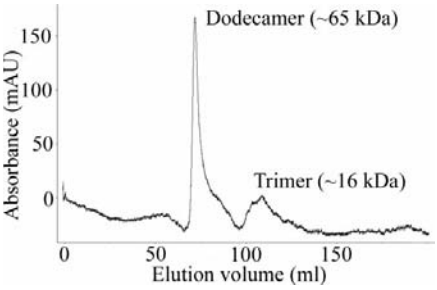

Figure 1
Gel-filtration elution profile of anti-TRAP.

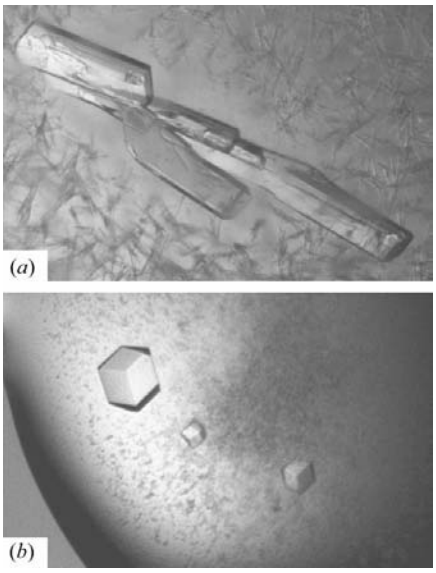

Figure 2
Crystals of anti-TRAP. (*a*) Plate-like crystals; (*b*) cubic shaped crystals.

resolution was identified. Interestingly, when the pH of the reservoir was increased to 8.0 (0.1 *M* triethanolamine), small cube-shaped crystals with dimensions of 0.2 × 0.2 × 0.2 mm appeared (Fig. 2*b*). These crystals produced limited diffraction to ∼8 Å resolution.

3.3. Data-collection statistics and self-rotation function analysis

X-ray data were collected to a resolution of 2.8 Å using a single crystal belonging to space group *P*1. Although the mosaicity was relatively high (1.6°), the data were processed and merged reasonably well. The main statistics of the data set are shown in Table 1.

To deduce the internal symmetry of anti-TRAP, we calculated the solvent content and analysed the self-rotation function $R(\Phi, \Psi, K)$ (Crowther, 1972). 12 monomers (four trimers), with a molecular weight of 12 × 5648 Da per asymmetric unit, result in a Matthews coefficient of 2.4 Å^3 Da^{-1} and a solvent content of 48% (Matthews, 1968). Three or five trimers of anti-TRAP per asymmetric unit would correspond to solvent contents of 61 and 35%, with Matthews coefficients of 3.2 and 1.9 Å^3 Da^{-1}, respectively.

The self-rotation function was calculated with a radius of integration of 30 Å using diffraction data within the 10.0–3.0 Å resolution shell. Peaks corresponding to four threefold axes (Fig. 3*a*) and three twofold axes (Fig. 3*b*) were observed. These peaks remained present when the radius of integration was varied. The constellation of peaks could be explained by four trimers arranged at the corners of a tetrahedron, as shown in Fig. 4. In that model, each trimer sits on a threefold axis, with twofold axes perpendicular to the faces of a cube.

The symmetry and gel-filtration data suggest that the anti-TRAP protein exists as a trimer or dodecamer in solution. Our data do not support the association of two trimers into a hexamer, as proposed previously on the basis of chemical cross-linking experiments (Valbuzzi & Yanofsky, 2002). In agreement with our results, data obtained recently by analytical ultracentrifugation (Snyder *et al.*, 2004) indicate that anti-TRAP exists as a dodecamer at high concentrations and as a trimer at low concentrations. It is reasonable to assume that physiological concentrations of anti-TRAP in the cell are lower than those required for association of trimers into dodecamers (subunit concentration of 12.5 µ*M* or higher). We therefore predict that anti-TRAP functions as a trimer.

The results reported here lay the groundwork for structure determination. The presence of one Zn atom per subunit should permit structure determination by the MAD technique.

Table 1
Data-collection statistics.

Values in parentheses are for the highest resolution shell.

Wavelength (Å)	0.87
Space group	*P*1
Unit-cell parameters (Å, °)	a = 51.6, b = 60.1, c = 60.4, α = 114.0, β = 101.4, γ = 100.5
Resolution (Å)	35–2.8 (2.95–2.8)
No. of measurements	26628 (458)
No. of unique reflections	13148 (229)
Completeness (%)	93.4 (82.2)
$R_{\rm merge}$† (%)	11.0 (18.6)
Average $I/\sigma(I)$	4.3 (3.4)
Multiplicity	1.9 (1.8)

† $R_{\rm merge} = \sum_h \sum_i |I(h)_i - \langle I(h)\rangle| / \sum_h \sum_i I(h)_i$, where $I(h)$ is the intensity of reflection h, $\sum_h$ is the sum over all measured reflections and $\sum_i$ is the sum over i measurements of a reflection.

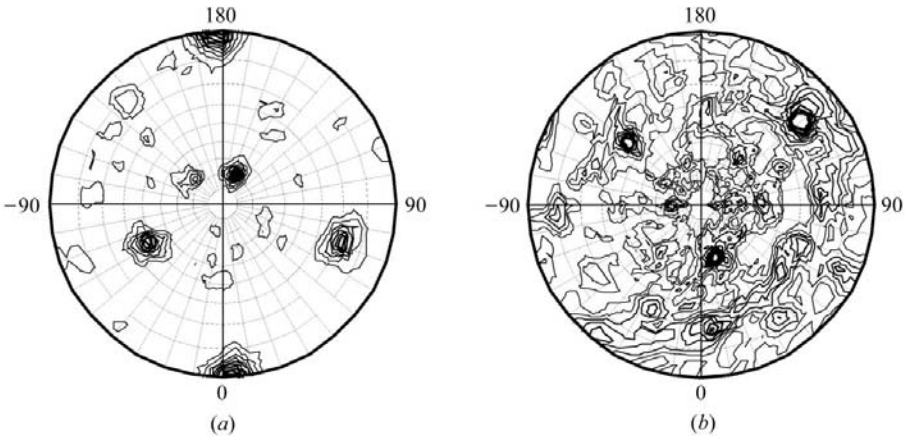

Figure 3
Stereographic projection of the self-rotation function, with the crystallographic *a* axis along $\varphi = 0°$, $\psi = 90°$ and the *c** axis perpendicular to the plane of the figure. The φ angle varies from 0 to ±180° around the plot, while the ψ angle varies from 0° at the centre to 90° at the edge of the ring. (*a*) Section with $\kappa = 120°$; (*b*) section with $\kappa = 180°$. The resolution of data used was 10.0–3.0 Å and the radius of integration was 30 Å. Contours start at the zero level and increase in 0.6σ intervals.

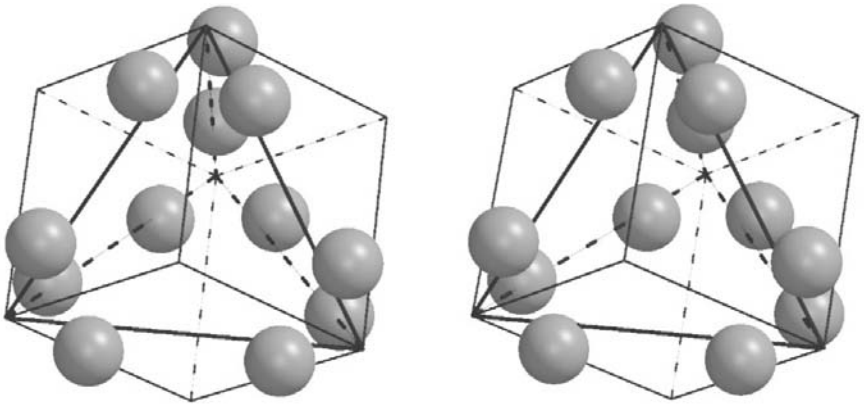

Figure 4
Stereo figure showing the arrangement of four trimers of anti-TRAP that constitute a crystallographically independent unit. Each monomer is represented by a sphere.

This work was supported by Wellcome Trust funds to MS and AA (grant No. 067416) and by National Institutes of Health and National Science Foundation funds to PG and YC (grants RO1GM62750 and MCB-9982652). We thank Andrey Lebedev for useful discussions. We also thank the Wellcome Trust for allocation of synchrotron beam time at Daresbury and Miroslav Papiz for help during the data collection.

References

Antson, A. A., Dodson, E. J., Dodson, G. G., Greaves, R. B., Chen, X. & Gollnick, P. (1999). *Nature (London)*, **374**, 693–700.
Antson, A. A., Otridge, J. B., Brzozowski, A. M., Dodson, E. J., Dodson, G. G., Wilson, K. S., Smith, T. M., Yang, M., Kurecki, T. & Gollnick, P. (1995). *Nature (London)*, **374**, 693–700.
Babitzke, P., Bear, D. & Yanofsky, C. (1995). *Proc. Natl Acad. Sci. USA*, **92**, 7916–7920.

Babitzke, P. & Gollnick, P. (2001). *J. Bacteriol.* **183**, 5795–5802.
Babitzke, P., Stults, J., Shire, S. & Yanofsky, C. (1994). *J. Biol. Chem.* **269**, 16597–16604.
Bradford, M. (1976). *Anal. Biochem.* **72**, 248–254.
Chen, X., Antson, A. A., Yang, M., Li, P., Baumann, C., Dodson, E. J., Dodson, G. G. & Gollnick, P. (1999). *J. Mol. Biol.* **289**, 1003–1016.
Collaborative Computational Project, Number 4 (1994). *Acta Cryst.* D**50**, 760–763.
Crowther, R. A. (1972). *The Molecular Replacement Method*, edited by M. G. Rossmann, pp. 173–185. New York: Gordon & Breach.
Evans, P. R. (1997). *Proceedings of the CCP4 Study Weekend. Recent Advances in Phasing*, edited by K. S. Wilson, G. Davies, A. W. Ashton & S. Bailey, pp. 97–102. Warrington: Daresbury Laboratory.
Gollnick, P. (1994). *Mol. Microbiol.* **11**, 991–997.
Gollnick, P. & Babitzke, P. (2002). *Biochim. Biophys. Acta*, **1577**, 240–250.
Hopcroft, N. H., Wendt, A., Gollnick, P. & Antson, A. A. (2002). *Acta Cryst.* D**58**, 615–621.
Jancarik, J. & Kim, S.-H. (1991). *J. Appl. Cryst.* **24**, 409–411.
Leslie, A. G. W. (1993). *Proceedings of the CCP4 Study Weekend. Data Collection and Processing*, edited by L. Sawyer, N. Isaacs & S. Bailey, pp. 44–51. Warrington: Daresbury Laboratory.
McElroy, C., Manfredo, A., Wendt, A., Gollnick, P. & Foster, M. (2002). *J. Mol. Biol.* **323**, 463–473.
McPherson, A. (1982). *Preparation and Analysis of Protein Crystals*, ch. 4, pp. 82–159. New York: Wiley.
Martinez-Yamout, M., Legge, G. B., Zhang, O., Wright, P. E. & Dyson, H. J. (2000). *J. Mol. Biol.* **300**, 805–818.
Matthews, B. W. (1968). *J. Mol. Biol.* **33**, 491–497.
Merino, E., Babitzke, P. & Yanofsky, C. (1995). *J. Bacteriol.* **177**, 6362–6370.
Snyder, D., Jeffrey, L., Chen, Y., Gollnick, P. & Cole, J. L. (2004). *J. Mol. Biol.* **338**, 669–682.
Vagin, A. & Teplyakov, A. (1997). *J. Appl. Cryst.* **30**, 1022–1025.
Valbuzzi, A., Gollnick, P., Babitzke, P. & Yanofsky, C. (2002). *J. Biol. Chem.* **277**, 10608–10613.
Valbuzzi, A. & Yanofsky, C. (2001). *Science*, **293**, 2057–2059.
Valbuzzi, A. & Yanofsky, C. (2002). *J. Biol. Chem.* **277**, 48574–48578.